

Exploring the Central Compact Object in the RX J0852.0-4622 Supernova Remnant with XMM-Newton

W. Becker¹, C. Y. Hui¹, B. Aschenbach¹, and A. Iyudin²

¹ Max-Planck Institut für Extraterrestrische Physik, Giesebachstrasse 1, D-85741 Garching, Germany

² Skobeltsyn Institute of Nuclear Physics, Moscow State University, Vorob'evy Gory, 119992 Moscow, Russia

Submitted to A&A on July 5, 2006

Abstract. The properties of the presumably young galactic supernova remnant (SNR) RX J0852.0-4622, discovered by ROSAT, are still uncertain. The data concerning the distance to the SNR, its age, and the presence of a compact remnant remain controversial. We report the results of several XMM-Newton observations of CXOU J085201.4-461753, the central compact source in RX J0852.0-4622. The currently preferred interpretation of CXOU J085201.4-461753 being a neutron star is in line with our analysis. The Chandra candidate pulsation periods are not confirmed; actually no period was found down to a 3σ upper limit for any pulsed fraction. The spectrum of CXOU J085201.4-461753 is best described by either a two blackbody spectrum or a single blackbody spectrum with a high energy power law tail. The two blackbody temperatures of 4 MK and 6.6 MK along with the small size of the emitting regions with radii of 0.36 and 0.06 km invalidate the interpretation that the thermal radiation is cooling emission from the entire neutron star surface. The double blackbody model suggests emission from the neutron star's hot polar regions. No X-ray lines, including the emission feature previously claimed to be present in Chandra data, were found.

Key words. Neutron Stars – Supernova Remnants – G266.2-1.2 – RX J0852.0-4622 – CXOU J085201.4-461753 – X-rays - XMM-Newton

1. Introduction

A very fascinating result reflecting the advantage of wide-field spectro-imaging observations provided by ROSAT in its all-sky survey (RASS) is the discovery of the supernova remnant RX J0852.0-4622 by Aschenbach (1998). The remnant is located along the line of sight towards the south-east corner of the Vela supernova remnant (cf. Fig.1). Because the latter dominates the emission in the soft band, RX J0852.0-4622 is best visible in the RASS data at energies above ~ 1 keV. The remnant has a circular shell-like shape with a diameter of 2 degrees. Although the distance to the remnant is uncertain, its free-expansion age ($t \sim 3.4 \times 10^3 v_{5k}^{-1} d_{1kpc}$ yr, with v_{5k} as expansion velocity in units of 5000 km/s) suggests a remnant age much younger than that of Vela. Because of its suggested age, it is often denoted as *Vela-Junior*.

COMPTEL data suggest that the remnant has a 1.157 MeV γ -line from the radioactive isotope ^{44}Ti associated with it (Iyudin et al. 1998). Together with ROSAT X-ray data, Aschenbach et al. (1999) suggested the remnant could be as young as ~ 680 years and as close as ~ 200 pc, which would make it the closest and youngest supernova

remnant among the ~ 231 galactic remnants known today (Green 2004).

However, reanalysis of COMPTEL data indicates that the detection of the ^{44}Ti line in the direction of RX J0852.0-4622 is only significant at the level of $\sim (2-4)\sigma$ (Schönfelder et al. 2000). Discarding the ^{44}Ti line detection would leave the age and distance estimates significantly less constrained. ASCA observations have shown that the hydrogen column absorption of the remnant is about one order of magnitude larger than that of the Vela supernova remnant (Tsunemi et al. 2000; Slane et al. 2001) which would suggest that RX J0852.0-4622 is far behind Vela. On the other hand, the lack of strong variation in the column absorption across RX J0852.0-4622 further indicates that the remnant cannot be more distant than the Vela Molecular Ridge, i.e. 1 to 2 kpc (Slane et al. 2001).

The X-ray spectra from RX J0852.0-4622 as obtained by the ASCA GIS detector are well described by a power law model which indicates that the X-ray emission of RX J0852.0-4622 is likely to be predominately non-thermal (Tsunemi et al. 2000; Slane et al. 2001). Together with SN1006 and G347.3-0.5, RX J0852.0-4622 thus forms the exclusive group of non-thermal shell-type supernova remnants which are believed to be accelerators of cosmic rays.

This is further supported by the recent detection of TeV γ -ray images by HESS which correlate well with the X-ray images (Aharonian et al. 2005).

Although the GIS spectra appear to be featureless and power law like, analysis of the spectrum of the north-western rim obtained by the ASCA SIS detector has shown a line feature at ~ 4.1 keV, though its significance was low (Tsunemi et al. 2000; Slane et al. 2001). The recent study of the rim of RX J0852.0-4622 with XMM-Newton has confirmed the non-thermal nature of the remnant as well as the presence of an emission line feature at 4.45 ± 0.05 keV (Iyudin et al. 2005). The authors suggest that the line (or lines) originate from the emission of Ti and Sc which might be excited by atom/ion or ion/ion high velocity collisions. This is in agreement with the width of the 1.157 MeV γ -ray line which indicates a large velocity of the emitting matter of ~ 15000 km/s (Iyudin et al. 1998). Furthermore, the consistency of the X-ray line flux and the γ -ray line flux support the existence and the amount of Ti in RX J0852.0-4622 claimed by Iyudin et al. (1998). However, if the interpretation of Iyudin et al. (2005) is correct, only sub-Chandrasekhar type Ia supernova can produce such high ejecta velocity within the current knowledge of explosion model. On the other hand a sub-Chandrasekhar type Ia supernova would not leave a compact stellar-like object, in contrast to the observations. Apart from the 1.157 MeV line, the decay chain $^{44}\text{Ti} \rightarrow ^{44}\text{Sc} \rightarrow ^{44}\text{Ca}$ also produces the hard X-ray lines at 67.9 keV and 78.4 keV. So far INTEGRAL observations have not found any evidence of these two lines (Renaud et al. 2006).

A central compact X-ray source CXOU J085201.4-461753 in RX J0852.0-4622 was first recognized as a 5σ excess in the RASS data by Aschenbach et al. (1998). Its existence was finally confirmed with the detection of a hard, somewhat extended X-ray source in the ASCA data (Tsunemi et al. 2000; Slane et al. 2001). To conclusively identify this source as the compact remnant of the supernova explosion that created RX J0852.0-4622 was not possible because of the presence of two foreground stars (HD 76060 and Wray 16-30) which could be responsible for at least part of the central X-ray emission. On the other hand, BeppoSAX observations have revealed another hard X-ray source, SAX J0852.0-4615, which was not resolved in previous observations (Mereghetti 2001). Based on its harder X-ray spectrum and higher X-ray to optical flux ratio, the authors found SAX J0852.0-4615 to be more likely a neutron star candidate associated with RX J0852.0-4622.

A first Chandra observation of the central part of Vela Jr was performed in October, 2000. The superior angular resolution of Chandra clearly resolved a point-like source, CXOU J085201.4-461753, and invalidated the association with the aforementioned foreground stars (Pavlov et al. 2001). Moreover, there was no source detected at the position of SAX J0852.0-4615. In view of this, there is little doubt that CXOU J085201.4-461753, located only ~ 4 arcmin off the geometric center of RX J0852.0-4622,

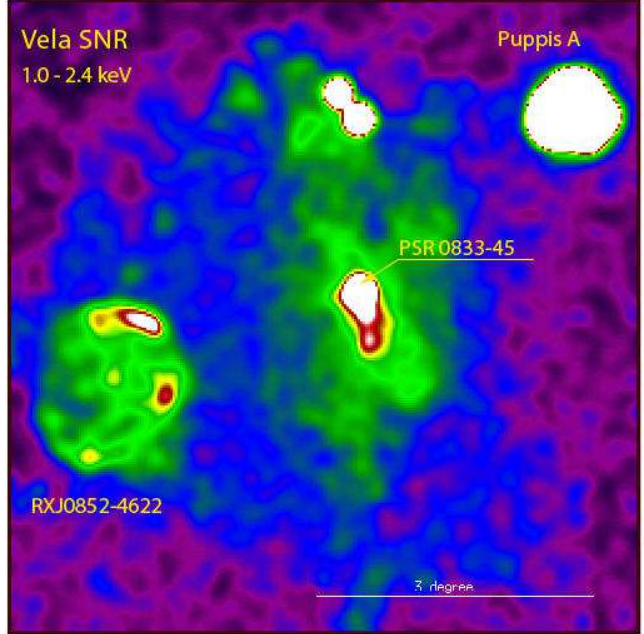


Fig. 1. *Vela and friends*: The two supernova remnants Puppis A and RX J0852.0-4622 are both located at the edge of the Vela supernova remnant. Emission from the central compact source CXOU J085201.4-461753 is clearly visible in the ROSAT all-sky survey image near to the center of RX J0852.0-4622.

is the compact remnant of the supernova explosion. This is further suggested by the f_x/f_{opt} ratio as the source has no optical counterpart known brighter than $m_B > 22.5$, $m_R > 21.0$ (Pavlov et al. 2001).

The first short 3 ksec Chandra observation provided only an accurate position for CXOU J085201.4-461753. Spectral analysis with this data were strongly hampered by low photon statistics and pile-up effect (Pavlov et al. 2001). A second 31.5 ksec Chandra observation performed in August, 2001, aimed for timing and spectral analysis and was set up in ACIS continuous clocking mode which provides 2.85 ms temporal resolution at the expense of spatial information in one dimension. In this data it was found that the spectrum of CXOU J085201.4-461753 can be well modeled by a single blackbody with a temperature of $\sim 4.68 \times 10^6$ K and a projected emitting area with a blackbody radius of ~ 280 m (Kargaltsev et al. 2002). From a timing analysis these authors reported two candidate periods of ~ 301 and ~ 33 ms, though the significance of these signals was rather low. Furthermore, no evidence for any long-term variability of the source flux was found (Kargaltsev et al. 2002).

Although there is no indication of diffuse nebular emission around the point source in X-rays (Pavlov et al. 2001; Kargaltsev et al. 2002), Pellizzoni, Mereghetti, & De Luca (2002) detected a faint and circular H_α nebula with a diameter of ~ 6 arcsec at the position of CXOU J085201.4-461753. These authors suggest that the nebula emission could be created by a bow shock which is driven by the relativistic wind of a neutron star.

Table 1. Details of XMM-Newton observations of CXOU J085201.4-461753. In the April 2001 observation CXOU J085201.4-461753 got placed right on a PN CCD gap. We therefore don't give a counting rate.

Detector	Instrument Mode	Filter	Start Date	Effective Exposure	Net Rate (cts s ⁻¹)
Obs. ID: 0112870601					
MOS1	Full Frame	Medium	2001-04-27	8 ksec	0.146 ± 0.004
MOS2	Full Frame	Medium	2001-04-27	8 ksec	0.149 ± 0.004
PN	Extended Full Frame	Medium	2001-04-27	6 ksec	
Obs. ID: 0147750101					
MOS1	Full Frame	Medium	2003-05-21	38 ksec	0.155 ± 0.002
MOS2	Full Frame	Medium	2003-05-21	38 ksec	0.156 ± 0.002
PN	Small Window	Thin	2003-05-21	25 ksec	0.477 ± 0.005
Obs. ID: 0147750201					
MOS1	Full Frame	Medium	2003-06-25	12 ksec	0.156 ± 0.004
MOS2	Full Frame	Medium	2003-06-25	12 ksec	0.154 ± 0.004
PN	Small Window	Thin	2003-06-25	8 ksec	0.472 ± 0.008

Many previous studies favor the interpretation of CXOU J085201.4-461753 being a neutron star. It should be admitted, though, that the properties of this compact object are not tightly constrained and hence its nature cannot be resolved without ambiguity. It is further still on discussion whether this source is physically associated with RX J0852.0-4622. Answering this question can help us to constrain the nature of RX J0852.0-4622 in turn.

In this paper, we present a first detailed study of CXOU J085201.4-461753 and its environment by making use all XMM-Newton data taken before 2005¹. In §2, we give a brief description of the performed observations. In §3, we present the methods and results of our data analysis which are subsequently discussed in §4.

2. Observations & Data Reduction

By early 2005 three observations have been targeted with XMM-Newton on CXOU J085201.4-461753. The basic information of the observations are summarized in Table 1. The huge collecting power and high spectral resolution of XMM-Newton provides us with data of much higher photon statistics than it was achieved with Chandra and other previous observatories.

CXOU J085201.4-461753 was first observed by XMM-Newton on April 27, 2001 for a duration of ∼ 25 ksec. The MOS1/2 and the PN cameras were operated in full-frame and extended full-frame mode, respectively. The medium filter was used in all instruments to block stray light and optical leakage from bright foreground stars. Since the accurate position of the central compact object was not known at the time of this first XMM-Newton observation, CXOU J085201.4-461753 got placed 2.3 arcmin off-axis. The point spread function at this off-axis angle is not much different from the on-axis one, but CXOU

J085201.4-461753 got located right on a CCD gap in the PN-camera, causing a severe decrease in photon statistics and data quality. We therefore excluded this PN dataset from our analysis.

The second and third XMM-Newton observations of CXOU J085201.4-461753 were performed on May 21, 2003 and June 25, 2003 with total exposure times of ∼ 43 and ∼ 17 ksec, respectively. CXOU J085201.4-461753 was observed on-axis in both observations. The MOS1/2 cameras were setup in the same way as in the 2001 observation. The EPIC-PN camera was operated in small-window mode with a thin filter.

All the raw data were processed with version 6.1.0 of the XMM Science Analysis Software (XMMSAS). We created filtered event files for the energy range 0.3 – 10 keV and selected only those events for which the pattern was between 0 – 12 for the MOS cameras and 0 – 4 for the PN camera. We further cleaned the data by accepting only good time intervals (when the sky background was low) and removed all events potentially contaminated by bad pixels. The effective exposure times after data cleaning and the background corrected source count rates in the 0.3 – 10 keV band are summarized in Table 1.

3. Data Analysis

3.1. Spatial Analysis

A false color image of the merged MOS1/2 data from all three XMM-Newton observations is displayed in Figure 2. CXOU J085201.4-461753 is the brightest source in the field. It is located at the western edge of a faint ∼ 9 × 14 arcmin wide diffuse and irregular shaped extended X-ray structure which emits mostly in the soft bands below ∼ 2 keV. The extended emission was already visible in ASCA images, but less resolved from and less discriminating the compact source because of ASCA's wide point

¹ Tentative results on the analysis of parts of this data were already published by Becker & Aschenbach (2002).

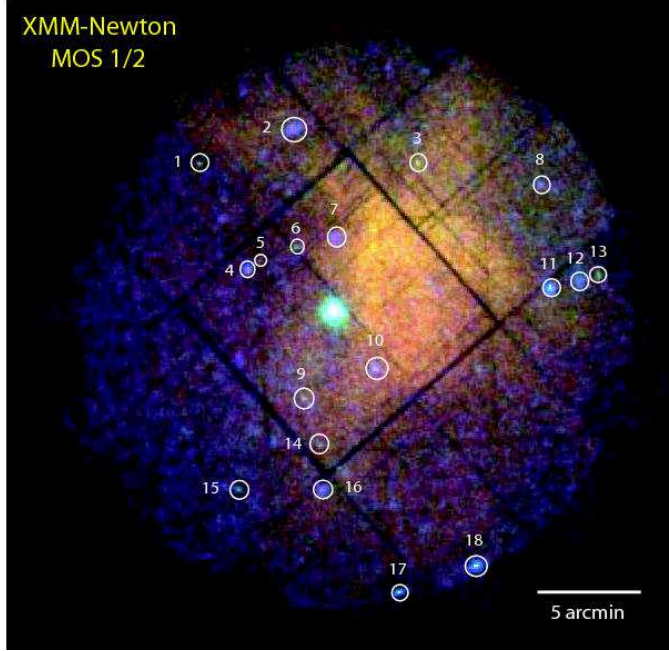


Fig. 2. XMM-Newton MOS1/2 false color image of the inner 30 arcmin central region of RX J0852.0-4622 (red: 0.3 – 0.75 keV; green: 0.75 – 2 keV and blue: 2 – 10 keV). The central bright source is CXOU J085201.4-461753. 18 other point-like sources, marked by circles, are detected in the field of view (cf. Table 2). The binning factor of this image is 4 arcsec.

spread function. The XMM-Newton observations provide for the first time a more detailed view of this field.

Apart from CXOU J085201.4-461753 we have detected 18 point-like sources serendipitously in the field of view. Their positions are given in Table 2. We have correlated these sources with the 30 radio sources discovered by Reynoso et al. (2006) within RX J0852.0-4622. We found that the nominal position of one of these radio sources coincides with the peak emission of the X-ray source 11. But cross-correlating all these 18 sources with SIMBAD and NED databases did not result in any identification within a circle of 30 arcsec radius around each source.

3.2. Spectral Analysis

As a compromise to select as much as possible events from CXOU J085201.4-461753 without the contamination from the surrounding remnant emission (see Figure 2) we extracted the source spectrum from a circular region of 20 arcsec radius. About 70% of all point source events are located within this region. Annular regions with radii of 22 and 35 arcsec, centered on CXOU J085201.4-461753, were used to extract the background spectra. The background corrected count rates are listed in column 6 of Table 1. Response files were computed for all datasets by using the XMMSAS tasks RMFGEN and ARFGEN. According to the XMMSAS task EPATPLOT, no dataset is affected by CCD pile.

Table 2. Faint X-ray sources detected serendipitously within RX J0852.0-4622.

Source	RA (J2000) h:m:s	Dec (J2000) d:m:s	δ RA arcsec	δ Dec arcsec
1	08:52:39.037	-46:10:50.08	0.45	0.31
2	08:52:12.931	-46:09:06.68	0.37	0.25
3	08:51:38.185	-46:10:46.41	0.38	0.26
4	08:52:25.433	-46:15:57.23	0.45	0.32
5	08:52:22.510	-46:15:28.37	0.50	0.48
6	08:52:11.708	-46:14:46.48	0.40	0.28
7	08:52:01.231	-46:14:18.78	0.31	0.21
8	08:51:04.275	-46:11:53.72	0.45	0.32
9	08:52:09.804	-46:22:04.49	0.38	0.26
10	08:51:49.975	-46:20:41.32	0.35	0.24
11	08:51:01.452	-46:16:47.83	0.30	0.23
12	08:50:53.378	-46:16:21.35	0.48	0.32
13	08:50:47.810	-46:16:09.15	0.45	0.33
14	08:52:04.977	-46:24:20.52	0.44	0.30
15	08:52:27.994	-46:26:25.81	0.78	0.28
16	08:52:04.651	-46:26:28.66	0.49	0.33
17	08:51:43.459	-46:31:22.22	0.50	0.28
18	08:51:22.030	-46:30:08.20	0.39	0.25

In order to fit spectra from all three observation runs simultaneously we have grouped the energy channels of all spectra dynamically. For the MOS1/2 data of the April 2001 observation we grouped the data with ≥ 30 counts/bin. For the MOS1/2 and PN data of the May 2003 observation we used a grouping with ≥ 100 counts/bin and ≥ 165 counts/bin, respectively, whereas for the June 2003 observations the MOS1/2 and PN data were grouped with ≥ 30 resp. 50 counts/bin. The different grouping reflects the differences in photon statistics in the various datasets.

All the spectral fits were performed in the 0.3 – 10 keV energy range by using XSPEC 11.3.1. The spectral models tested include a single blackbody, a double blackbody, a power law, a combination of a blackbody and power law model as well as a broken power law and a thermal bremsstrahlung model. The parameters of all fitted model spectra are summarized in Table 3. The quoted errors are conservative and are 1σ for 2 parameters of interest for single component spectral models and for 3 parameters of interest for multi-component models.

A single blackbody model gives a parameter set of $T = (4.53 \pm 0.05) \times 10^6 K$, $R = 0.29 \pm 0.01$ km (for a distance $d = 1$ kpc) and $N_H = 3.22^{+0.14}_{-0.13} \times 10^{21} \text{ cm}^{-2}$ ($\chi^2_{\nu} = 1.21$ for 431 dof). These values are similar to those inferred from Chandra data by Kargaltsev et al. (2002). However, with a more than 3 times improved photon statistic we find that this simple model cannot describe the data beyond ~ 3 keV and hence a single blackbody is not a valid description for the spectrum of CXOU J085201.4-461753. This is in contradiction to the results obtained by Kargaltsev et al. (2002) using Chandra data only.

Adding a second thermal component improves the fit and represents very well the observed spectrum up to ~ 7 keV (see Figure 3). This thermal multi-component model yields a parameter set of $N_H = 3.82^{+0.36}_{-0.30} \times 10^{21}$

cm^{-2} , $T_1 = (2.98^{+0.28}_{-0.47}) \times 10^6 \text{ K}$, $R_1 = 0.36^{+0.05}_{-0.03} \text{ km}$, $T_2 = (6.60^{+3.02}_{-1.18}) \times 10^6 \text{ K}$ and $R_2 = 59^{+64}_{-43} \text{ m}$ ($\chi^2_\nu = 1.08$ for 429 dof). R_1 and R_2 are given for a distance of 1 kpc. The F -test statistic indicates that the improvement of the goodness-of-fit for adding an extra thermal spectral component is significant at a confidence level of $\geq 99\%$. To further constrain the parameter space for this two component thermal model we calculated the χ^2_ν error contours which are shown in Figure 4. We would like to point out that the column density derived by us is consistent with the results from the spectral analysis of RX J0852.0-4622 by Iyudin et al. (2005).

We have also tested whether there is any thermal emission contributed from an emission area compatible with the entire neutron star surface. However, with R_1 fixed to 10 km we found that the goodness-of-fit decreased significantly to $\chi^2_\nu = 1.46$ (for 430 dof).

Testing non-thermal emission models shows that a single power law model cannot fit the data ($\chi^2_\nu = 2.18$ for 431 dof). However, a model combining a blackbody and a power law yields a goodness-of-fit which is comparable with that obtained with the double blackbody model ($\chi^2_\nu = 1.09$ for 429 dof). The inferred slope of the power law component is Γ is $4.21^{+0.30}_{-0.59}$. A similar steep slope has also been observed in the X-ray spectrum of the central compact X-ray source RX J0822-4300 in Puppis-A (Hui & Becker 2006). We point out that such a steep power law slope, a priori, cannot be considered to be *unphysical* as the nature of the central compact object is still uncertain. Compared with the double blackbody model the column density of the combined blackbody plus power law model, $N_H = 7.63^{+0.72}_{-1.59} \times 10^{21} \text{ cm}^{-2}$, is higher. However, we find it still within the limit of the total Galactic neutral hydrogen column density along the direction to CXOU J085201.4-461753 ($\sim 10^{22} \text{ cm}^{-2}$; Dickey & Lockman 1990). The uncertainty in the source distance thus does not support to reject the blackbody plus power law model because of a larger N_H value.

We have also examined whether a thermal bremsstrahlung model, which physically implies that the central compact object is surrounded by a hot plasma, yields a viable description. χ^2_ν and N_H resulting from this model are similar to the values inferred from the broken power law and hence cannot be considered as an appropriate description of the source spectrum (c.f. Table 3).

From the October 2001 Chandra observation Kargaltsev et al. (2002) reported a marginal detection of a spectral feature at 1.68 keV with a width of ~ 100 eV. The authors found that the shape of this feature is similar to that of an inverse P Cygni profile, suggesting a mass accreting neutron star. However, we have not found any significant feature around 1.68 keV in the spectra obtained by XMM-Newton. Figure 3b shows the contribution of the χ^2 statistics in the $\sim 1.6 - 1.8$ keV range for the best-fitted double blackbody model. There is no evidence for any systematic residual in this region. In order to quantify this result we have fitted a

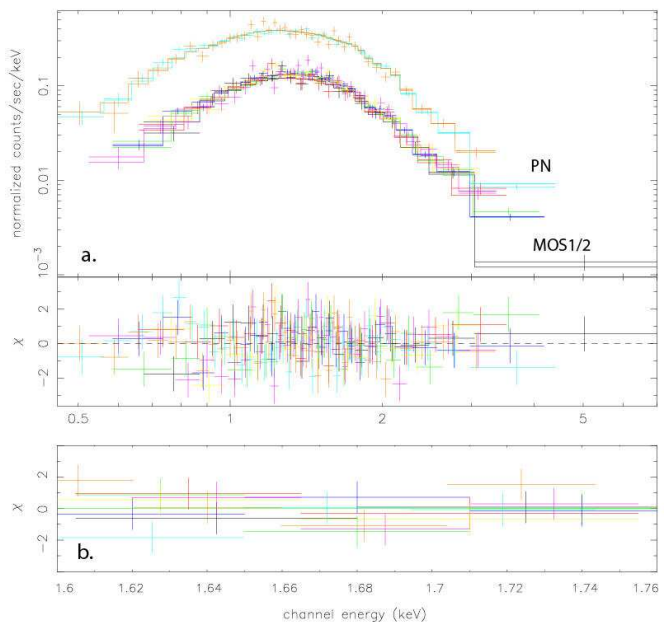


Fig. 3. **a.** Energy spectra of CXOU J085201.4-461753 observed with the EPIC-PN (upper spectra) and the MOS1/2 detectors (lower spectra) with the best-fitting absorbed two component blackbody model (*upper panel*), and the contribution to the χ^2 fit statistic (*lower panel*). **b.** Details of the χ^2 fit distribution of the absorbed two component blackbody model in the $\sim 1.6 - 1.8$ keV energy range. No line feature is indicated in the fit residuals.

Gaussian line of width 100 eV at 1.68 keV. A 3σ upper limit of such a Gaussian line is 8.27×10^{-6} photons $\text{cm}^{-2} \text{ s}^{-1}$, or 2.23×10^{-14} erg $\text{cm}^{-2} \text{ s}^{-1}$.

3.3. Timing Analysis

The May and June 2003 observations were performed with the EPIC-PN camera operated in the small-window mode. The 5.7 ms temporal resolution provided by that mode enables us to search for coherent pulsations in these datasets. For the timing analysis we selected all events within $0.3 - 10$ keV from a circle of 25 arcsec centered on the CXOU J085201.4-461753. This yields 15668 and 5974 events. The background contribution in each observation is about 15%.

The barycentric corrections of the arrival times were performed with the XMMSAS task BARYCEN. The position of CXOU J085201.4-461753 measured by Chandra, RA= $8^{\text{h}}52^{\text{m}}01^{\text{s}}.38$ and Dec= $-46^{\circ}17'53''.34$ (J2000), was used for barycentering photon arrival times in both datasets.

A FFT based period search did not reveal any strong signal of pulsed emission. Taking the candidate periods found by Kargaltsev et al. (2002), $P = 300.8214531$ ms and $P = 32.92779028$ ms, as initial trials, we carried out a detailed search around these periods by using the Z_m^2 test where m is the numbers of harmonics included (Buccheri et al. 1983). We did not find any promising signals around

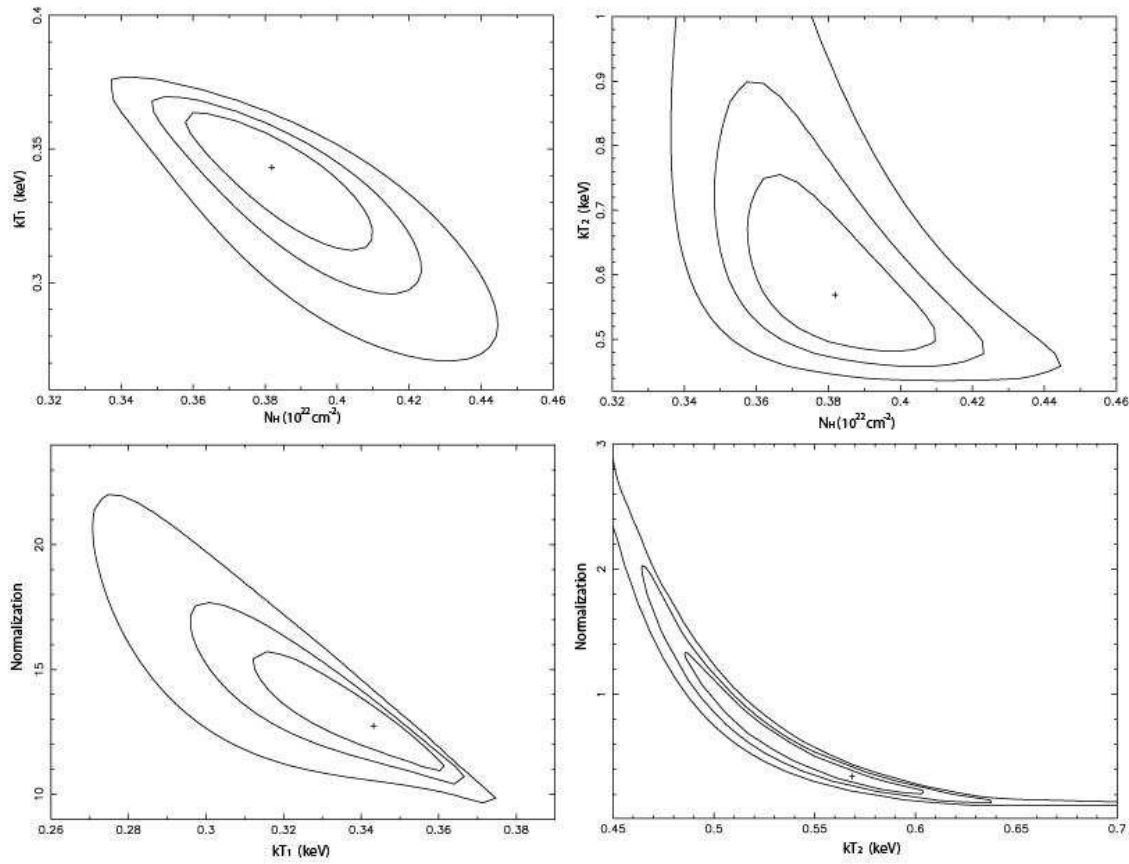


Fig. 4. 1σ , 2σ and 3σ confidence contours for the double blackbody fit to the X-ray spectrum of CXOU J085201.4-461753.

these test periods either. A pulsed fraction upper limit p was computed using the May 2003 data according to

$$n_\sigma = \frac{p \sqrt{N_{tot}}}{\sqrt{p + \frac{d}{1-d} (1-p)}}$$

in which N_{tot} is the total number of detected source counts (12871 cts), p is the pulsed fraction (fraction between pulsed and total counts) and d is the duty cycle (fraction between pulsed and total time interval). Assuming a duty cycle of $d = 0.5$ (sinusoidal modulation) we compute for $n_\sigma = 3$ a pulsed fraction upper limit of $p \sim 3\%$.

4. Discussion

We have observed the neutron star CXOU J085201.4-461753 in the supernova remnant RX J0852.0-4622 with XMM-Newton. The XMM data have invalidated the interpretation that the nature of the diffuse and extended emission surrounding CXOU J085201.4-461753 is plerionic and powered by the young neutron star. The spectrum of CXOU J085201.4-461753 is best fitted by a double blackbody spectrum or a blackbody plus non-thermal spectral component. The fitted temperatures along with the small size of the emitting regions invalidate the interpretation that the thermal radiation is cooling emission from the entire neutron star surface. If the double black-body model

indeed is the right description for the emission scenario of CXOU J085201.4-461753 it points towards emission from a $\sim 4 - 6.5$ MK hot polar-region on the neutron star surface.

In the literature various models are proposed to produce hot-spots on the neutron star surface. Almost all magnetospheric emission models predict a bombardment of the polar cap regions by energetic particles accelerated in the magnetosphere backwards to the neutron star surface (cf. Cheng, Ho & Ruderman 1982; Harding & Muslimov 2002 and references therein). Though CXOU J085201.4-461753 is not known to be a radio pulsar it still could be possible that the hot polar caps are heated by particle bombardment while the radio emission itself is undetected due to an unfavorable beaming geometry. This is not an unlikely scenario. The opening angle of a radio beam is inversely proportional to the square-root of the pulsar's rotation period so that the radio beams of slow rotating pulsars can easily miss the observers line of sight and thus keep undetected.

The heat transport in neutron stars is accomplished by electrons and positrons. A strong magnetic field thus is expected to have an essential impact on the neutron star cooling as it channels the heat along the magnetic field lines and suppresses it perpendicular to it. Neutron star cooling with a full treatment of the strong magnetic

field thus should lead to an anisotropic heat flow and subsequently to an anisotropic surface temperature distribution, with the polar-cap regions getting hotter than the surface temperature of the equatorial regions. This scenario has been modeled recently by Geppert et al. (2004; 2006).

Independent of these scenarios there exists the possibility that CXOU J085201.4-461753 is accreting from fall-back matter or a residual disk and that the accreting matter causes the hot-spots on the surface.

The low pulsed fraction upper limit is not in disagreement with any of these scenarios. When general relativistic effects are taken into account (Page 1995; Hui & Cheng 2004), pulsations are found to be strongly suppressed and the pulsed fraction is highly dependent on the mass to radius ratio of the star, the orientation of the hot spot and the viewing angle geometry. This is due to the fact that the gravitational bending of light will make more than half of the stellar surface become visible at any instant and hence the contribution of the hot spot will be strongly reduced. If the orientation of the hot spot differs from that of an orthogonal rotator and/or the star has a high mass to radius ratio, then very low amplitude pulsations are expected.

Anyway, future data to be taken in forthcoming observations will further explore the emission models and hopefully detect the neutron star's rotation period.

Acknowledgements. The XMM-Newton project is an ESA Science Mission with instruments and contributions directly funded by ESA Member States and the USA (NASA). The XMM-Newton project is supported by the Bundesministerium für Wirtschaft und Technologie/Deutsches Zentrum für Luft- und Raumfahrt (BWI/DLR, FKZ 50 OX 0001), the Max-Planck Society and the Heidenhain-Stiftung.

References

Aharonian, F., Akhperjanian, A. G., Bazer-Bachi, A. R., et al. 2005, A&A, 437, L7

Aschenbach, B., 1998, Nature, 396, 141

Aschenbach, B., Iyudin, A., Schönfelder, V., 1999, A&A, 350, 997

Becker, W., Pavlov, G.G., 2001, in *The century of Space Science*, eds. Bleeker et al., Kluwer Academic Press

Buccheri, R., et al. 1983, A&A, 128, 245

Cheng, K.S., Ho, C. & Ruderman, M.A., 1986, ApJ, 300, 500

Geppert, U., Küker, M., Page, D., 2004, A&A, 426, 26

Geppert, U., Küker, M., Page, D., 2006, A&A submitted, astro-ph/0512530

Green D.A., 2004, 'A Catalogue of Galactic Supernova Remnants (2004 January version)', Mullard Radio Astronomy Observatory, Cavendish Laboratory, Cambridge, United Kingdom

Harding, A.K., Muslimov, A.G., 2002, ApJ, 568, 862

Hui, C.Y. & Becker, W., 2006, A&A in press (arxiv:astro-ph/0508655)

Hui, C. Y., & Cheng, K. S. 2004, ApJ, 608, 935

Iyudin, A. F., Aschenbach, B., Becker, W., Dennerl, K., & Haberl, F. 2005, A&A, 429, 225

Iyudin, A. F., Schönfelder, V., Bennet, K., et al. 1998, Nature, 396, 142

Kargaltsev, O., Pavlov, G. G., Sanwal, D., & Garmire, G. P. 2002, ApJ, 580, 1060

Mereghetti, S., 2001, ApJ, 548, L213

Page, D. 1995, ApJ, 442, 273

Pavlov, G.G., Sanwal, D., Kiziltan, B., G.Garmire, 2001, ApJ, 559, 131

Pellizzoni, A., Mereghetti, S., & De Luca, A. 2002, A&A, 393, L65

Renaud, M., Vink, J., Decourchelle, A., Lebrun, F., Terrier, R., & Ballet, J. 2006 (arxiv:astro-ph/0602304)

Reynoso, E. M., Dubner, G., Giacani, E., Johnston, S., & Green, A. J., 2006, A&A, 449, 243

Schönfelder, V., Bloemen, H., Collmar, W., et al. 2000, AIP Conf. Proc, AIP, 510, 54

Slane, P., Hughes, J.P., Edgar, J., et al., 2001, ApJ, 548, 814

Tsunemi, H., Miyata, E., Aschenbach, B., Hiraga, J., Akutsu, D., 2000, PASJ, 52, 887

Zavlin, V.E., Pavlov, G.G., Shibanov, Y.A., 1996, A&A, 315, 141

Parameter	BB	BB+BB	BB+BB (fix R_1 at 10 km)	PL	BB+PL	BKPL	BREMSS
$N_H (10^{21} \text{ cm}^{-2})$	$3.215^{+0.135}_{-0.132}$	$3.819^{+0.356}_{-0.295}$	$9.212^{+0.313}_{-0.553}$	10.994	$7.633^{+0.718}_{-1.594}$	$7.422^{+0.421}_{-0.519}$	$6.821^{+0.146}_{-0.156}$
Γ_1	-	-	-	4.407	$4.208^{+0.298}_{-0.590}$	$3.050^{+0.170}_{-0.213}$	-
Γ_2	-	-	-	-	-	$5.139^{+0.238}_{-0.188}$	-
$T_1 (10^6 \text{ K})$	$4.533^{+0.048}_{-0.049}$	$3.983^{+0.281}_{-0.466}$	$1.358^{+0.022}_{-0.042}$	-	$4.248^{+0.114}_{-0.147}$	-	$9.874^{+0.201}_{-0.178}$
$T_2 (10^6 \text{ K})$	-	$6.599^{+3.023}_{-1.177}$	$4.171^{+0.054}_{-0.066}$	-	-	-	-
$R_1 (\text{km})$	$0.285^{+0.009}_{-0.008}$	$0.357^{+0.052}_{-0.034}$	10	-	$0.300^{+0.034}_{-0.021}$	-	-
$R_2 (\text{km})$	-	$0.059^{+0.064}_{-0.043}$	$0.408^{+0.018}_{-0.014}$	-	-	-	-
$F_{X_{0.5-10keV}} (\text{ergs cm}^{-2} \text{ s}^{-1})$	1.905×10^{-12}	2.113×10^{-12}	9.916×10^{-12}	1.720×10^{-11}	6.324×10^{-12}	5.426×10^{-12}	4.162×10^{-12}
Reduced χ^2	1.208	1.083	1.460	2.177	1.094	1.200	1.207
D.O.F	431	429	430	431	429	429	431

Table 3. Spectral model parameters of CXOU J085201.4-461753 derived from XMM-Newton data; models: blackbody (BB), two blackbodies (BB+BB), power law (PL), blackbody plus power law (BB+PL), broken power law (BKPL), bremsstrahlung (BREMSS).